Hindawi
Advances in Civil Engineering
Volume 2019, Article ID 3279586, 11 pages
https://doi.org/10.1155/2019/3279586

Research Article

Sandstone Dynamical Characteristics Influenced by Water-Rock Interaction of Bank Slope

Huafeng Deng, Yinchai Zhang, Yongyan Zhi, Lingling Duan, Jianlin Li, Xushu Sun, and Xiaoliang Xu

Key Laboratory of Geological Hazards on Three Gorges Reservoir Area (China Three Gorges University), Ministry of Education, Yichang, Hubei, China

Correspondence should be addressed to Huafeng Deng; dhf8010@ctgu.edu.cn

Received 28 November 2018; Accepted 11 February 2019; Published 19 March 2019

Academic Editor: Claudio Mazzotti

During the long-term reservoir operation, the seismic capability and dynamic response characteristics of the bank slope are of great importance to its safety evaluation content. Aimed at typical bank slopes, considering reservoir water level fluctuation and soaking-air drying cyclic interaction, an experiment has been designed and conducted. In addition, the cyclic loading test with different stress amplitudes was carried out in different water-rock cycles. The laboratory results indicate that (1) during the immersion-air dry circulation process, the damping ratio and damping coefficient of sandstone gradually increased while the dynamic elastic modulus decreased. It is obvious that the dynamic elastic modulus of sandstone decreases dramatically during the immersion-air dry circulation process, especially in the first six periods. Also, its variation curve fits with the logarithmic curve. (2) When the cyclic load stress amplitude increases from 10 MPa to 35 MPa, the damping ratio and coefficient of the rock sample gradually decreased while dynamic elastic modulus increased. each dynamic parameter shows a more obvious variation trend when the stress amplitude is lower than 25 MPa. (3) During the water-rock interaction process, the closely knit microstructure of rock gradually becomes loose and porous, which resulted in the degradation of macroscopic physical and mechanical properties of sandstone. (4) In the analysis of the seismic response of the bank slope, the actual water-rock interaction process and the seismic level of the bank slope should be more considered. To find out further accurate reflection in the earthquake resistance and dynamic response of the bank slope, it is necessary to select the reasonable dynamic parameter to carry out seismic research.

1. Introduction

According to the operation requirements of the Three Gorges reservoir, the water level of the reservoir fluctuates between 145 m and 175 m each year after its completion, which generates the hydro-fluctuation belt with 30 m height between the two sides of the 600 km long channel. Since the Three Gorges reservoir impoundment in June 2003, the frequency of earthquake in this area has increased greatly and numerous microearthquakes have been detected in or around the reservoir. The earthquake occurred in Zigui County is considered as an example. It occurred on December 16, 2013, with an earthquake magnitude of 4.1, focal depth of 8 km, and epicenter intensity degree of IV. Analysis indicates that its recorded seismic waveform has a long period with more low-frequency components and less high-frequency components. On December 16, 2013, a 5.1 magnitude earthquake occurred in Badong County of the Three Gorges reservoir area, with a depth of 5.0 km, located at the place which is 100 kilometers from the Three Gorges dam. It was the largest earthquake since impoundment of the Three Gorges reservoir. Except for deformation and damage of hydraulic structures, reservoir earthquake also generates adverse effects on the safety of the bank slopes.

In the long-term operation of the reservoir, the water-rock interaction significantly influences the physical and mechanical properties of the bank slope [1]. The elastic modulus, uniaxial compressive strength, cohesion, and internal friction angle of sandstone were reduced in different degrees under the dry-wet circulation [2, 3]. A series of dry-

wet cycling tests were carried out on sandstone, shale, and mud stone [4–9], whose results indicated that the dry-wet cycle causes irreversible progressive damage to the rock. Jeng et al. [10] and Lin et al. [11] found the microscopic mechanism of sandstone degradation under the dry-wet circulation. Combined with self-designed rock soak device YRK-1, the water-rock test considering changes in water pressure and soaking-air drying cycle was carried out which indicated that water-rock damage effect become more obvious when the soaking water pressure changes increased. According to the tentative analysis on rock dynamic characteristics under water-rock interaction, with the increase of immersion-air dry circulation [12], the rock's damping coefficient and damping ratio increased gradually while the dynamic elastic modulus decreased.

The study shows that, in the long-term running process of reservoir, water-rock interaction leads to static and dynamic characteristics gradual degradation of rock mass so as to change the dynamic response characteristics of the bank slope under the geological process. As seen from the current monitoring data, the earthquakes occurred vary greatly in magnitude in the Three Gorges reservoir area, with most magnitude of 3 to 4 and minor of 4 to 5. In sense, the actual dynamic load amplitude of the bank slope rock mass is not a fixed value but a changed one in a certain range. Besides, stress amplitude has significant effect on the rock dynamic characteristics [13, 14]. Dynamic response analysis of bank slope is an important part of reservoir design and its safety evaluation. In order to learn better about the seismic capacity and the dynamic response rule of bank slope under the long-time reservoir water fluctuation, it is important to consider water-rock interaction and dynamic loading amplitude influence, as well as the selection of reasonable dynamic parameter. However, the present study pays less attention to the water-rock interaction influence and cyclic load stress on the rock dynamic characteristics.

In the periodical fluctuation process of the reservoir water level, some rock bodies in the hydro-fluctuation belt zone are in dry and wet circulation with especially serious water-rock effect. As shown in Figure 1, the rock mass destruction is obvious in the zone, which means the hydro-fluctuation belt is a sensitive zone to the water-rock interaction of the bank slope [15, 16]. Based on the sandstone creep behaviors under the coupling effects of seepage pressure and stress, a nonlinear nonstationary plastic-viscous creep model which can describe the curve of sandstone creep tests is proposed [17]. To quantify the rate of change of rock mechanical properties, a modified Hoek–Brown failure criterion was proposed, in which a new parameter was introduced to model the cumulative damage to rocks after water saturation-dehydration circulation [18]. In consequence, we selected rock mass of the typical bank slope hydro-fluctuation belt in the Three Gorges reservoir area as the research object. To simulate realistic environmental conditions, the water-rock interaction test considering water pressure changes and soaking-air drying circulation was carried out to analyze the influence of long-term water-rock interaction on the dynamic characteristics of sandstone.

Figure 1: Rock mass destruction photo of typical bank slope hydro-fluctuation belt zone.

2. Test Design and Calculation Principle

2.1. Sample Preparation. Originating from the bank slope of the Three Gorges reservoir area, known for its weak weathering medium-grained quartz identification, this sandstone was selected as the research object in this paper. According to the standard requirements [19], the standard rock samples with a diameter of 50 mm and height of 100 mm are prepared. After the longitudinal wave velocity and mass measurement, the rock samples with relative concentration of wave velocity and density are selected as test samples [20]. Typical test rock samples are shown in Figure 2.

2.2. Water-Rock Interaction Test Scheme. In view of the actual environment conditions of the bank slope in the Three Gorges reservoir area, the self-developed YRK-2 rock immersion-air dry circulation test instrument shown in Figure 3 was used to simulate the water pressure fluctuation and soak-air dry cycle process. The single water-rock cycle lasts 40 days and is divided into 2 stages: the first stage is the drying stage, during which the sample is soaked in a container with the constant temperature of 35°C (the simulation process of drying during low water level) and then air-dried for 10 days; the second stage is the soaking period, during which firstly the samples are soaked in a container filled with water for 10 days, during that time water pressure increases to 0.3 MPa for 10 days (simulating water level rise from 145 m to 175 m) and then the water pressure remains unchanged for 10 days (simulating water stability in the 175 m), and in the end, the water pressure reduces uniformly to 0 within the last 10 days (simulating water level decrease from 175 m to 145 m). Then, repeat the above soak-air dry procedure, and the total design cycle is 10 times. For the study of the dynamic characteristics of sample degradation rule at different water-rock cycles, cyclic loading and unloading tests and uniaxial compression test were performed on a set of the sample selected separately at the end of 1st, 2nd, 4th, 6th, 8th, and 10th cycle of soaking.

2.3. Cyclic Loading and Unloading Test Scheme. The uniaxial compressive strength of the rock sample is 80 Mpa under saturated state, and the grading loading and unloading test was carried out with the lower load stress of 5 Mpa. For this test, stress upper limit (σ_{max}) was designed for 15, 20, 25, 30,

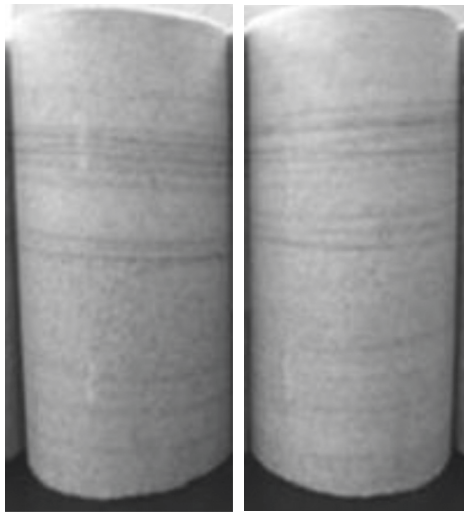

Figure 2: Typical test sample photo.

(a) (b)

Figure 3: YRK-2 rock soaking-air drying test device. (a) Soaking container. (b) Control cabinet.

35, and 40 MPa, respectively, while stress amplitude ($\Delta\sigma$) was designed for 10, 15, 20, 25, 30, 35 MPa, and each designed load cycle lasts 10 times with the frequency of 0.2 Hz. After the grading cyclic loading and unloading process, the axial load is applied to the rock sample for entire damage. The typical rock sample stress-strain curve is shown in Figure 4.

2.4. Calculation Principle of Rock Dynamic Parameters. In the unloading and unloading circulation process, the stress-strain curve often shows obvious nonlinear distribution due to the nonideal elastic medium of rock. And, the unloading curve is below the loading curve with hysteresis loop composed of the dynamic stress-strain curve. As is shown in Figure 5, the size of the loop area reflects the energy dissipated during a loading and unloading process. Damping ratio, damping coefficient, and dynamic elastic modulus are defined in the following equations:

$$\lambda = \frac{A_R}{4\pi A_S},$$

$$C = \frac{A_R}{\pi X^2 \omega}, \tag{1}$$

$$E_d = \frac{\sigma_{dmax} - \sigma_{dmin}}{\varepsilon_{dmax} - \varepsilon_{dmin}}.$$

In these equations, σ_{dmax} and σ_{dmin} denote, respectively, the maximum and minimum dynamic stress in dynamical stress-strain hysteresis loop while ε_{dmax} and ε_{dmin} denote the

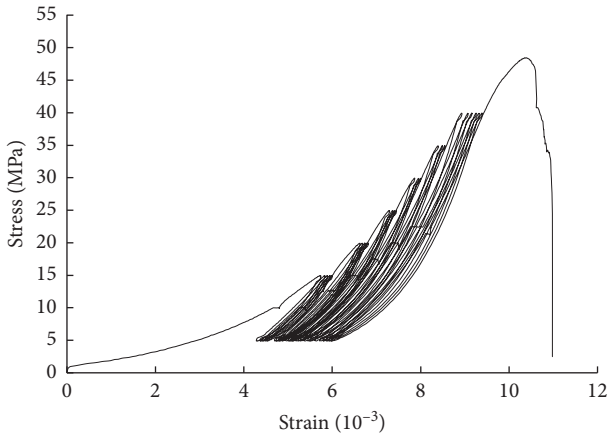

Figure 4: Typical rock sample stress-strain curve for cycle loading and unloading.

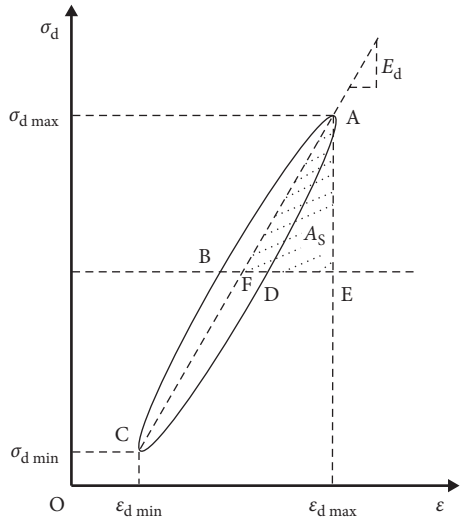

Figure 5: Hysteresis loop of dynamic strain and stress.

maximum and minimum dynamic strain, respectively. A_R represents the area of hysteresis loop ABCDA; A_S refers to the area of triangle AEF, and $4A_S$ reflects the maximum elastic strain energy the rock reserves in a cycle; X is the response amplitude, and ω is the circular frequency of loading and unloading.

3. Analysis of the Sandstone Dynamic Stress-Strain Curve under the Water-Rock Interaction

The stress-strain curve of the typical rock sample in different immersion-air dry circulation is shown in Figure 6.

As seen from Figure 6, the rock sample stress-strain curves share general coherent variation trend during different immersion-air dry circulations. However, with the increase of the dry-wet cycle, under the same cyclic load stress amplitude, the strain amplitude gradually increases and the corresponding hysteresis loop gradually tilts to the strain-increasing direction. The area of hysteresis loop also

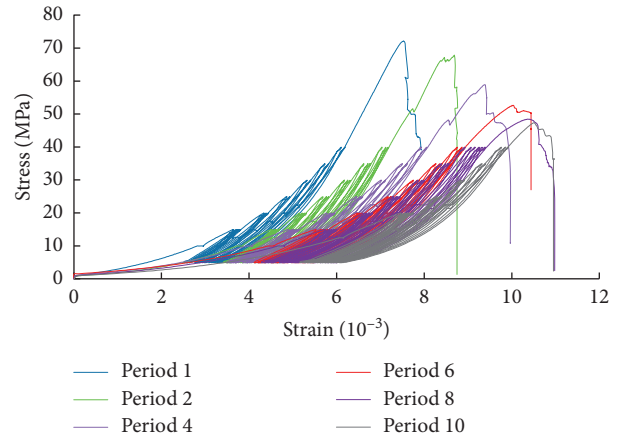

Figure 6: Typical rock sample stress-strain curve in different water-rock cycles.

increased, so did the corresponding axial strain at the end of grading loading and unloading process.

After the grading cyclic loading and unloading process, the axial load is applied to the rock sample for entire damage to get its curve of compressive strength. At the same time, the uniaxial compression test was carried out in different immersion-air dry circulations for comparative analysis and the compressive strength deterioration curve of the rock sample is shown in Figure 7.

Figure 7 shows that the compressive strength of rock samples decreases gradually with the increase of immersion-air dry circulation, and it shows conspicuous deterioration tendency in the first six immersion-air dry circulations. As the immersion-air dry circulation increased from 1 to 10, the uniaxial compressive strength of rock samples decreased by 26.81% while the compressive strength of grading loading and unloading decreased by 35.34%. The compressive strength of rock samples is relatively less than that of the uniaxial compression test during the same immersion-air dry circulation periods, and the disparity of the two became more obvious as the immersion-air dry circulation increased. It turns out that the graded cyclic load of rock samples shows obvious cumulative damage effect as the immersion-air dry circulation increased.

In order to calculate the dynamic parameters of the rock sample, the loop area is calculated in Figure 6. For the comparison analysis of the calculation results, the sixth hysteresis loop in the 10 cycles of each level is selected to calculate. The statistics of A_R and A_S in different immersion-air dry circulations are shown in Figure 8 separately.

As is depicted in Figure 8, the variation curves of A_R and A_S fit with logarithmic function as the immersion-air dry circulation increased. As the immersion-air dry circulation increased from 1 to 10, A_R with corresponding stress amplitudes of 10, 15, 20, 25, 30, 35, and 40 MPa rises to 129.67%, 94.90%, 86.07%, 79.27%, 74.93%, and 69.74% while A_S rises to 93.47%, 37.55%, 30.66%, 25.96%, 24.99%, and 23.39%. The curves of A_R and A_S grew fast during the first 6 immersion-air dry circulations and then gradually tend to be slow; besides, the smaller the stress amplitude of cyclic load, the more obvious the growth trend of A_R and A_S.

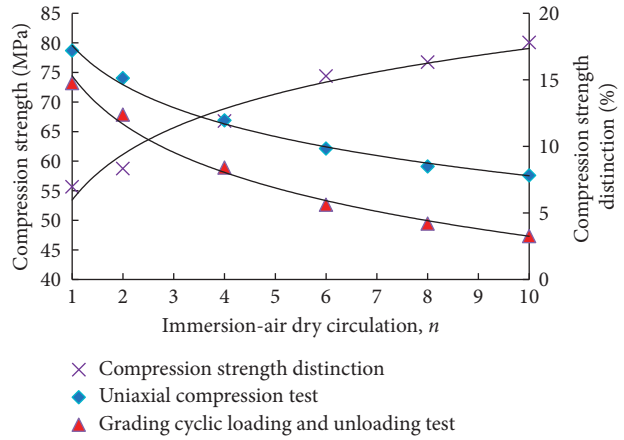

Figure 7: The compressive strength deterioration curve of rock sample under water-rock interaction.

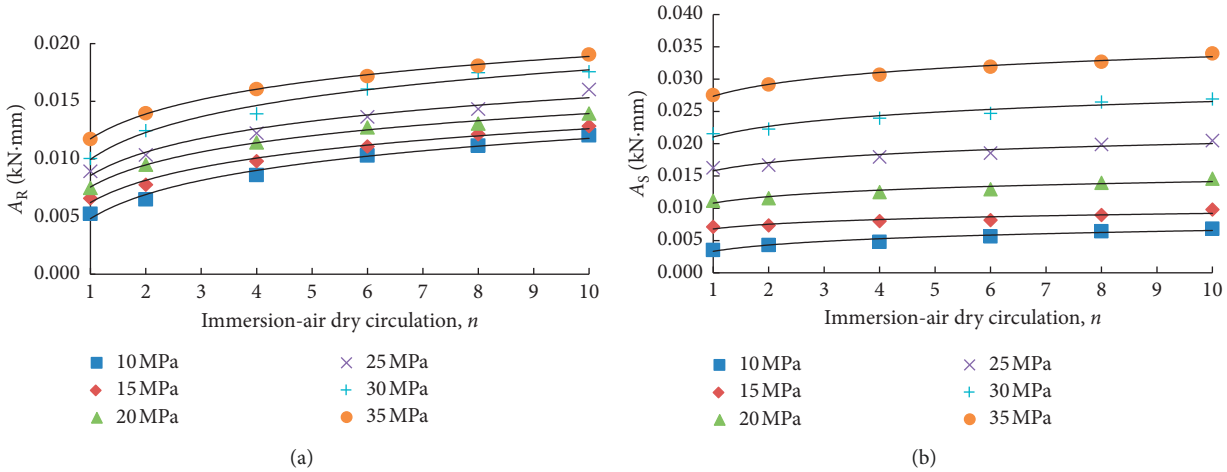

Figure 8: The variation curves of A_R and A_S under water-rock cycle. Variation curves of (a) A_R and (b) A_S.

4. Analysis of Sandstone Dynamical Parameters Variation Rule under Water-Rock Interaction

4.1. Damping Ratio. The damping ratio variation curves of rock sample under immersion-air dry circulation are as Figure 9.

As is depicted in Figure 9(a), the damping ratio curve of the rock sample increases gradually under the immersion-air dry circulation, which is in the form of logarithmic function. During the first 6 cycles' stage, damping ratio corresponding with diverse stress amplitude increased 36.37% to 19.95%, and it increased 42.39% to 28.19% at the end of the 10th cycle. The curves of damping ratio grew fast during the first six water-rock cycles and then gradually tended to be slow.

As is shown in Figure 9(b), the damping ratio curve of the rock sample decreases gradually as the stress amplitude increased, which is in the form of power function. When stress amplitude of cycle loading rose from 10 to 35 MPa, the damping ratio of rock samples in different water-rock cycles decreases 61.80% to 77.14%, respectively. The damping ratio of rock samples in different immersion-air dry circulations is larger at low stress amplitude. When the stress amplitude is more than 25 MPa, the damping ratio decreases slowly than that of before and the gap in damping ratio of rock samples between varied water-rock cycles narrows down gradually.

4.2. Damping Efficient. The damping factor variation curves of the rock sample under immersion-air dry circulation are shown in Figure 10.

As is depicted in Figure 10(a), the damping factor curve of the rock sample increases gradually under the immersion-air dry circulation, which is in the form of logarithmic function. During the first 6 cycles' stage, the damping factor corresponding with diverse stress amplitude increased 35.13% to 49.86%, and it increased 50.34% to 65.79% at the end of the 10th cycle. The curves of damping ratio grew fast during the first 6 water-rock cycle and then gradually tended to be slow.

As is shown in Figure 10(b), the damping factor curve of the rock sample decreases gradually as the stress amplitude increased, which is in the form of power function. When stress amplitude of cycle loading rose from 10 to 35 MPa, the damping factor of rock samples in different water-rock cycles decreases 24.68% to 33.33%, respectively. The damping factor of rock samples in different immersion-air dry circulations is

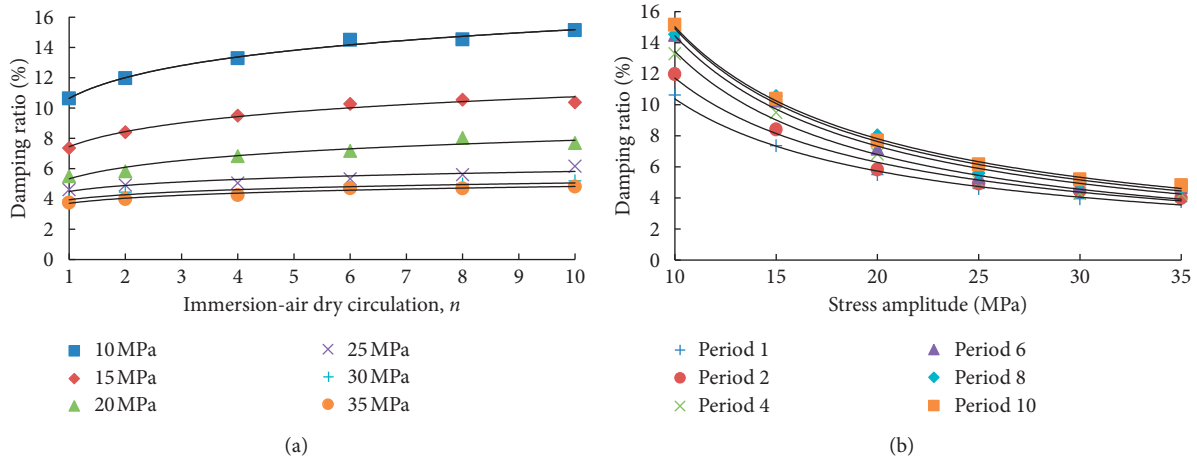

Figure 9: Damping ratio variation curves of the rock sample under water-rock interaction. (a) The relation curve of damping ratio with water-rock cycle. (b) The relation curve of damping ratio with cyclic load stress amplitude.

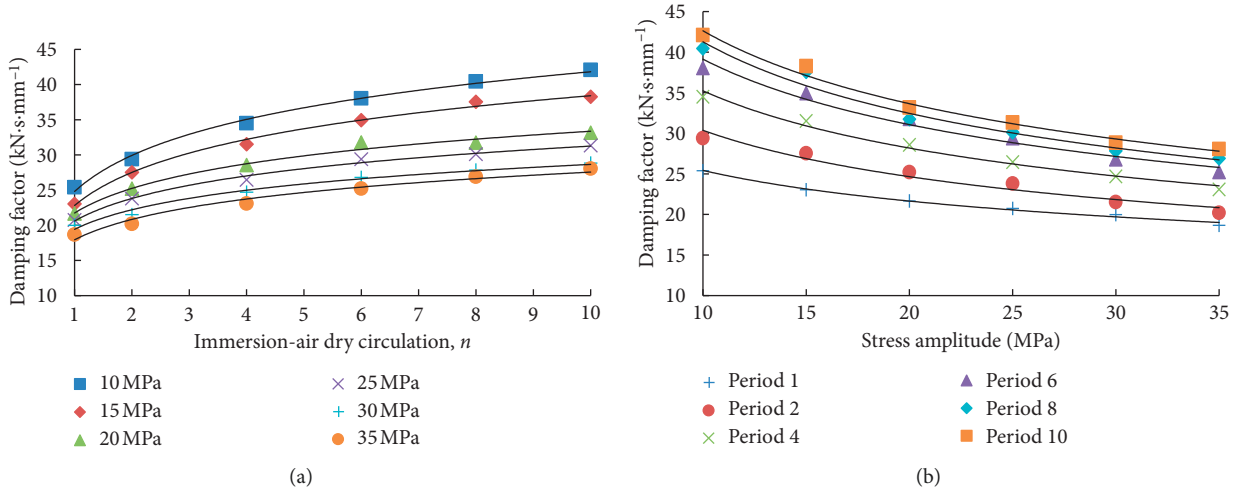

Figure 10: Damping factor variation curves of the rock sample under water-rock interaction. (a) The relation curve of damping factor with water-rock cycle. (b) The relation curve of damping factor with cyclic load stress amplitude.

larger at low stress amplitude. When the stress amplitude is over 25 MPa, the damping factor slowly decreases.

4.3. Dynamic Modulus of Elasticity. The dynamic elasticity modulus variation curves of the rock sample under immersion-air dry circulation are shown in Figure 11.

As is depicted in Figure 11(a), the dynamic elasticity modulus curve of the rock sample decreases gradually under the immersion-air dry circulation, which is in the form of logarithmic function. During the first 6 cycles' stage, the dynamic elasticity modulus corresponding with diverse stress amplitude decreased 18.35% to 38.34%, and it decreased 26.18% to 48.78% at the end of the 10th cycle. The curves of dynamic elasticity modulus decreased fast during the first six water-rock cycles and then gradually tended to be slow.

As is shown in Figure 11(b), the dynamic elasticity modulus curve of the rock sample decreases gradually as the stress amplitude increased, which is in the form of logarithmic function. When stress amplitude of cycle loading rose from 10 to 35 MPa, the dynamic elasticity modulus of rock samples in different water-rock cycles increases from 25.81% to 74.51%, respectively. The dynamic elasticity modulus of rock samples is larger at low stress amplitude. When the stress amplitude is more than 25 MPa, the dynamic elasticity modulus will increase slowly.

5. Analysis of Sandstone Microstructure Change Rule under Water-Rock Interaction

Composed of mineral grains skeleton, pore, and cranny, rock is a typical kind of heterogeneous material. Under the effect of immersion-air dry circulation, rock structure of mineral grains and pores change continually, which affects its physical and mechanical property [21] Therefore, the microstructure of rock samples was analyzed by SEM in different water-rock cycles as shown in Figure 12. And, the magnification diameter of SEM photos is 1200 scales of the original.

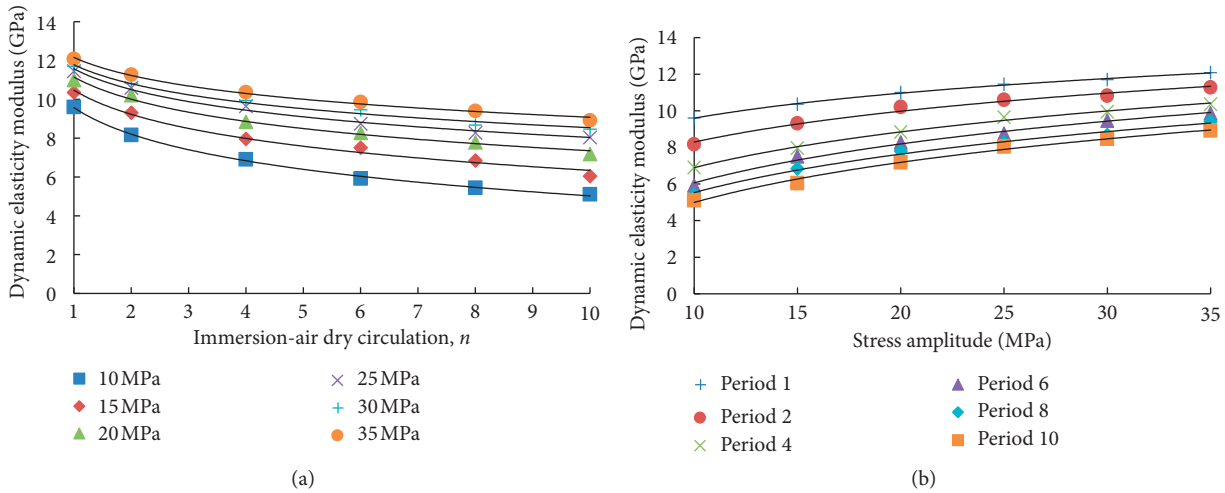

Figure 11: Dynamic elasticity modulus variation curves of the rock sample under water-rock interaction. (a) The relation curve of dynamic modulus of elasticity with water-rock cycle. (b) The relation curve of dynamic modulus of elasticity with cyclic load stress amplitude.

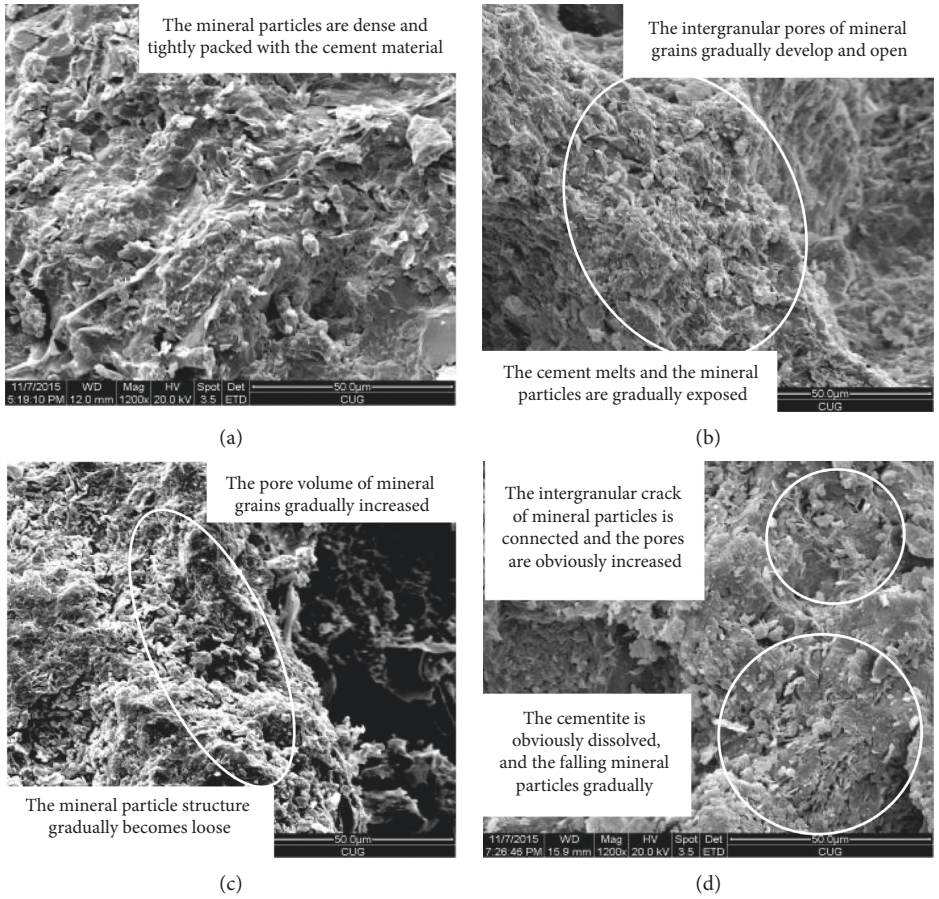

Figure 12: Continued.

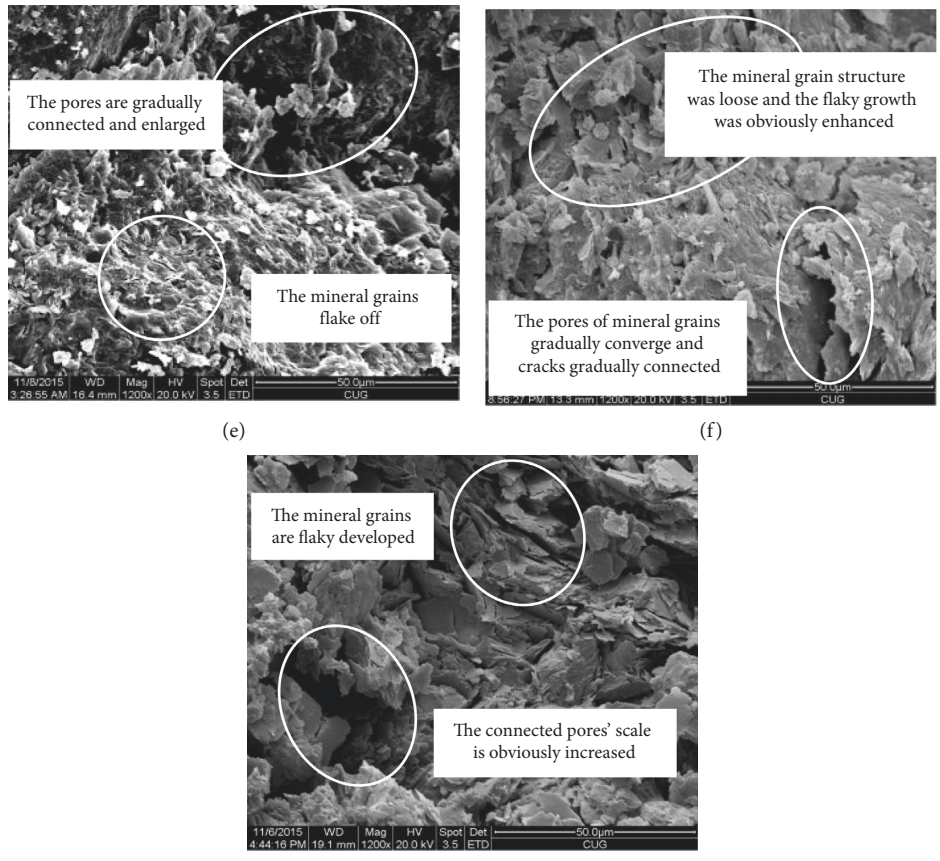

Figure 12: Microstructure characteristics of rock samples under the water-rock interaction (×1200). (a) The original state. (b) The first period. (c) The second period. (d) The fourth period. (e) The sixth period. (f) The eighth period. (g) The tenth period.

As seen from Figure 12, sandstone structure variation of mineral grains and pores stands out in the immersion-air dry circulation.

As is shown in Figure 12(a), the mineral particles in the rock sample were originally closely packed and tightly packed with the cement material.

As is shown in Figure 12(b), after the first cycle of immersion-air dry circulation, the calcareous cement between mineral grains gradually dissolved while mineral particles gradually became prominent with the increased pores between the mineral particles.

As is shown in Figure 12(c), after the second cycle of immersion-air dry circulation, some mineral particles were exposed to the space that was around the dissolved cementing material, and the granular structure tended to be loose. The local pores between mineral grains developed gradually.

As is shown in Figure 12(d), after the third cycle of immersion-air dry circulation, mineral particles were no longer closely surrounded by cementing material due to its further dissolution and the connection between particles became loose, with microcracks and obvious developed secondary porosity along the boundaries in the mineral grains.

As is shown in Figure 12(e), after the sixth cycle of immersion-air dry circulation, the original pores in the rock sample were further developed and opened and the cracks between the mineral particles gradually expanded and connected, forming a large pore channel, and some mineral particles were flaked.

As is shown in Figure 12(f), after the eighth cycle of immersion-air dry circulation, the microcracks and pores in the mineral grains gradually increased and converged and the mineral grains were developed obviously.

As is shown in Figure 12(g), after the tenth cycle of immersion-air dry circulation, the mineral particles without cement packed gradually decomposed into thin sheets. The intergranular pores gradually converged with the pore size increased significantly.

For the quantitative analysis of sandstone porosity change rule under water-rock action, the porosity of rock sample test was carried out and the results are shown in Figure 13.

As seen from Figure 13, the porosity of rock sample increased gradually as water-rock cycle proceeded, with the prime 3.27% and 4.26% to 4.42% in the sixth and tenth cycle. The curve of the porosity grew fast during the first six water-rock cycles and then gradually tended to be slow, which is the same as that of dynamical parameters. It means that the increasing trend of rock sample porosity shares the same trend of the pore structure in the SEM photos.

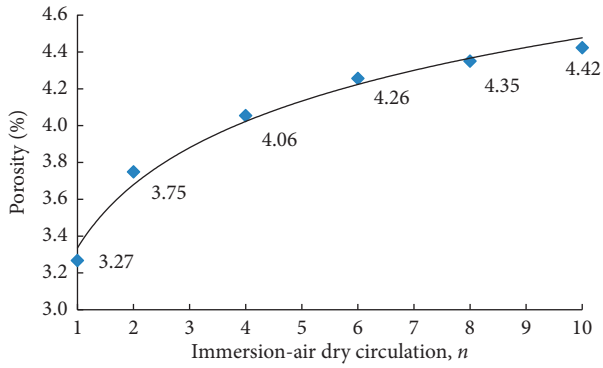

Figure 13: Porosity curve of rock sample under water-rock interaction.

6. Analysis of Deterioration Mechanism of Sandstone Mechanical Properties under Water-Rock Interaction

The sandstone is mainly composed of quartz, feldspar and cuttings, and porous calcareous cementation with a large number of microscopic cracks inside. During the process of pressure soaking, water molecules infiltrate, and on the one hand, it makes rock minerals and cement lubricate melted, resulting in soft mineral skeleton; on the other hand, the calcareous cement is deliquescent, and feldspar minerals are partially dissolved which produces new secondary minerals [22, 23]. After that, soluble substances with the water molecules movement enter into the soaked solution, while insoluble mineral precipitated at internal microcracks in rock mass generates crystal pressure, which promotes growth of the internal microscopic fracture. During the process of air-drying and drop soaking water pressure, secondary minerals move outward with water molecule extravasation, which results in further promoted micropores and provides more new reaction surfaces for the next water-rock physics and chemistry cycle.

At the same time, during the fluctuated process of water pressure, stress concentration is generated in the crack tip, which induces crack propagation and aggregation. It is beneficial to the water molecules seepage channel formation in the rock sample, which leads to the increasing porosity of the rock sample.

The water-rock interaction of bank slope is a process of the dry-wet cycle mentioned above. This includes the process of the sample microcrack development, extension, and collection, and the original tight microstructure becomes loose. It also results in the degradation of rock physical and mechanical properties.

There are many factors that affected the rock dynamical characteristics, among which the strength of mineral skeleton and development degree of micropores dominate. With the skeleton of the rock softened, the porosity gradually increased in the process of water-rock interaction. Under the same stress amplitude of cyclic loading, both the axial strain amplitude and irreversible plastic deformation of the sample increased, with the corresponding hysteresis loops inclined to increased strain direction, resulting in the degradation of dynamic parameters.

In the cyclic loading and unloading experiments, six stress amplitudes, including 10, 15, 20, 25, 30, and 35, were considered. At low stress amplitude, the sample's microfracture inside affects hysteresis loop shape significantly under the cyclic loading action, resulting in obvious variation between dynamic parameters of different water-rock cycles. As the stress amplitude of cyclic load increased, the microscopic defects in the rock sample gradually closed and so did the dynamic parameters variation.

During the early stage of the water-rock interaction, the calcium cement dissolution contributed a lot to the porosity development of rock. Besides, the cracks on the surface of the relative "fresh" mineral particles possessed higher activation energy, resulting in faster water-rock physical chemistry process and degradation trend of physical and mechanical parameters of rock sample. As the water-rock interaction cycles increased, the number of soluble calcareous cements decreased obviously and so did the activation energy on the surface of cracks and mineral particles. At the same time, the surfaces of the mineral grains were covered with secondary minerals produced by various feldspars, reducing the range of the water-rock interaction. All these factors above influence the process of water-rock interaction, which leads to the slow physical and chemical action process as well as the same deterioration tendency of the related physical and mechanical parameters.

7. Conclusions

The following conclusions were made based on the findings of this paper:

(1) During the whole process of immersion-air dry circulation, the damping ratio of sandstone increases gradually while the damping coefficient and dynamic elastic modulus decrease. As a result, the variation curves share the logarithmic form with distinct changes through the first six cycles.

(2) The stress amplitude of cyclic load affected greatly on the rock sample's dynamic characteristics. When the stress amplitude rose from 10 MPa to 35 MPa, the damping ratio and damping coefficient of the rock sample both decrease, while the dynamical plastic modulus increases. The variation trend of each dynamic parameter is more obvious when the stress amplitude is lower than 25 MPa.

(3) During the immersion-air dry circulation process of bank slope, mineral particles gradually dissolved and a series of physical and chemical actions took place in feldspars, which leads to the softened skeleton of rock mineral grains. With the microcrack development and fissures converge, the rock mineral grain structures become loose and porous. All these changes in microstructure lead to the deterioration of macroscopic physical and mechanical properties of sandstone.

(4) With the increase of the water-rock interaction period, the internal pores and fractures of the rock sample developed gradually, and the stress amplitude of cyclic load has a greater effect on dynamical parameters of the rock sample.

(5) During the long-term operation of the Three Gorges reservoir, on the one hand, the water-rock interaction by the fluctuated water level leads to the dynamic characteristics deterioration of the rock mass in the bank slope; on the other hand, due to the diverse magnitude of frequent reservoir earthquake, the rock mass of bank slope suffered varied dynamical loads, with different dynamical responses generated, respectively. Therefore, in the earthquake response analysis of the bank slope, it is supposed to consider the actual water-rock process and the level of earthquake as well as the selection of reasonable dynamic calculation parameters, for the calculation results better accord with the actual situation of the slope.

Nomenclature

σ_{max}: Maximum dynamic stress of dynamic stress-dynamic strain hysteresis curve
σ_{min}: Minimum dynamic stress of dynamic stress-dynamic strain hysteresis curve
ε_{dmax}: Maximum dynamic strain of dynamic stress-dynamic strain hysteresis curve
ε_{dmin}: Minimum dynamic strain of dynamic stress-dynamic strain hysteresis curve
A_R: Area of ABCD in the hysteresis loop
A_S: Area of the triangle AEF
E_d: Dynamic elastic modulus of the rock sample.

Data Availability

All data generated or analyzed during this study are included in this article and its supplementary information files.

Conflicts of Interest

The authors declare that there are no conflicts of interest regarding the publication of this paper.

Acknowledgments

This work was supported by the National Nature Science Foundation of China (No. 51679127), Key Laboratory of Geological Hazards on Three Gorges Reservoir Area (China Three Gorges University), Ministry of Education Open Fund Project (No. 2018KDZ04), and National Nature Science Foundation of China (No. 51439003); it was also sponsored by Research Fund for Excellent Dissertation of China Three Gorges University (Grant no. 2018SSPY023).

Supplementary Materials

The data used to support the findings of this study are included within the supplementary information file. (*Supplementary Materials*)

References

[1] S. J. Wang, F. S. Ma, and Y. L. Du, "On the rock-water interaction in reservoir areas and its geo environmental effect," *Journal of Engineering Geology*, vol. 4, no. 3, pp. 1–9, 1996, in Chinese.

[2] X. R. Liu, Y. Fu, Y. X. Wang et al., "Deterioration rules of shear strength of sand rock under water-rock interaction of reservoir," *Chinese Journal of Geotechnical Engineering*, vol. 30, no. 9, pp. 1298–1302, 2008, in Chinese.

[3] X. R. Liu, L. Zhang, and Y. Fu, "Experimental study of mechanical properties of argillaceous sandstone under wet and dry cycle in acid environment," *Rock and Soil Mechanics*, vol. 35, no. 2, pp. 45–52, 2014, in Chinese.

[4] P. A. Hale and A. Shakoor, "A laboratory investigation of the effects of cyclic heating and cooling, wetting and drying, and freezing and thawing on the compressive strength of selected sandstones," *Environmental and Engineering Geoscience*, vol. 9, no. 2, pp. 117–130, 2003.

[5] C. Apollaro, L. Marini, T. Critelli, and R. De Rosa, "The standard thermodynamic properties of vermiculites and prediction of their occurrence during water-rock interaction," *Applied Geochemistry*, vol. 35, pp. 264–278, 2013.

[6] M. Tallini, B. Parisse, M. Petitta, and M. Spizzico, "Long-term spatio-temporal hydrochemical and 222Rn tracing to investigate groundwater flow and water-rock interaction in the Gran Sasso (central Italy) carbonate aquifer," *Hydrogeology Journal*, vol. 21, no. 7, pp. 1447–1467, 2013.

[7] P. Alt-Epping, L. W. Diamond, M. O. Häring, F. Ladner, and D. B. Meier, "Prediction of water-rock interaction and porosity evolution in a granitoid-hosted enhanced geothermal system, using constraints from the 5 km Basel-1 well," *Applied Geochemistry*, vol. 38, pp. 121–133, 2013.

[8] J. A. Hurowitz and W. W. Fischer, "Contrasting styles of water-rock interaction at the mars exploration rover landing sites," *Geochimica et Cosmochimica Acta*, vol. 127, pp. 25–38, 2014.

[9] H. Y. Yao, Z. H. Zhang, and C. H. Zhu, "Experimental study of mechanical properties of sandstone under cyclic drying and wetting," *Rock and Soil Mechanics*, vol. 31, no. 12, pp. 3704–3708, 2010, in Chinese.

[10] F. S. Jeng, M. L. Lin, and T. H. Huang, "Wetting deterioration of soft sandstone—microscopic insights," in *Proceedings of an International Conference on Geotechnical and Geological Engineering*, p. 525, Melbourne, VIC, Australia, November 2000.

[11] M. L. Lin, F. S. Jeng, L. S. Tsai, and T. H. Huang, "Wetting weakening of tertiary sandstones-microscopic mechanism," *Environmental Geology*, vol. 48, no. 2, pp. 265–275, 2005.

[12] H. F. Deng, M. L. Zhou, J. L. Li, X. S. Sun, and Y. L. Huang, "Creep degradation mechanism by water-rock interaction in the red-layer soft rock," *Arabian Journal of Geosciences*, vol. 9, no. 12, pp. 1–12, 2016, in Chinese.

[13] H. F. Deng, X. F. Yuan, L. H. Wang et al., ""Experimental research on changes in the mechanical property law of reservoir bank sandstone under "immersion-air dry" circulation," *Environmental Engineering and Management Journal*, vol. 12, no. 9, pp. 1785–1789, 2013, in Chinese.

[14] H. F. Deng, Q. Luo, and J. L. Li, "Dynamic characteristics deterioration laws of sandstone under cyclic saturation-air drying," *Rock and Soil Mechanics*, vol. 34, no. 9, pp. 2468–2474, 2013, in Chinese.

[15] J. F. Liu, Y. W. Zhai, J. L. Pei et al., "Experimental study on dynamic characteristics of marble specimens under cyclic

loadings with different frequencies," *Journal of Henan Polytechnic University (Natural Science)*, vol. 33, no. 4, pp. 432–436, 2014, in Chinese.

[16] M. M. He, N. Li, Y. S. Chen et al., "An experimental study of dynamic behaviors of rock under stepwise cyclic loading," *Rock and Soil Mechanics*, vol. 36, no. 10, pp. 2907–2913, 2015, in Chinese.

[17] X. Wang, Y. Yin, J. Wang, B. Lian, H. Qiu, and T. Gu, "A nonstationary parameter model for the sandstone creep tests," *Landslides*, vol. 15, no. 7, pp. 1377–1389, 2018.

[18] X.-G. Wang, J.-D. Wang, T.-F. Gu, and B.-Q. Lian, "A modified Hoek-Brown failure criterion considering the damage to reservoir bank slope rocks under water saturation-dehydration circulation," *Journal of Mountain Science*, vol. 14, no. 4, pp. 771–781, 2017.

[19] The National Standards Compilation Group of People's Republic of China GB/T 50266-2013, *Standard for Tests Method of Engineering Rock Masses*, China Planning Press, Beijing, China, 2013, in Chinese.

[20] H. F. Deng, J. L. Li, C. J. Deng et al., "Analysis of sampling in rock mechanics test and compressive strength prediction methods," *Rock and Soil Mechanics*, vol. 32, no. 11, pp. 3399–3403, 2011, in Chinese.

[21] Y. C. Zhang, H. F. Deng, W. Wang, L. Duan, Y. Zhi, and J. Li, "The dynamic response law of bank slope under water-rock interaction," *Advances in Civil Engineering*, vol. 2018, Article ID 1306575, 10 pages, 2018.

[22] W. G. Li, X. P. Zhang, and Y. M. Zhong, "Formation mechanism of secondary dissolved pores in arose," *Oil & Gas Geology*, vol. 26, no. 2, pp. 220–223, 2005.

[23] H. F. Deng, J. L. Li, K. W. Wang et al., "Research on secondary porosity changing law of sandstone under saturation-air dry cycles," *Rock and Soil Mechanics*, vol. 33, no. 2, pp. 483–488, 2012, in Chinese.